Experimental and theoretical investigation of the electronic structure of Cu2O and CuO thin films on Cu(110) using x-ray photoelectron and absorption spectroscopy

Peng Jiang, David Prendergast, Ferenc Borondics, Soeren Porsgaard, Lisandro Giovanetti et al.

Citation: J. Chem. Phys. **138**, 024704 (2013); doi: 10.1063/1.4773583
View online: http://dx.doi.org/10.1063/1.4773583
View Table of Contents: http://jcp.aip.org/resource/1/JCPSA6/v138/i2
Published by the American Institute of Physics.

Experimental and theoretical investigation of the electronic structure of Cu_2O and CuO thin films on Cu(110) using x-ray photoelectron and absorption spectroscopy

Peng Jiang,[1,a)] David Prendergast,[2] Ferenc Borondics,[3,b)] Soeren Porsgaard,[4] Lisandro Giovanetti,[1,c)] Elzbieta Pach,[1] John Newberg,[3,d)] Hendrik Bluhm,[3] Flemming Besenbacher,[4] and Miquel Salmeron[1,5,e)]

[1]*Materials Sciences Division, Lawrence Berkeley National Laboratory, Berkeley, California 94720, USA*
[2]*The Molecular Foundry, Materials Sciences Division, Lawrence Berkeley National Laboratory, Berkeley, California 94720, USA*
[3]*Chemical Sciences Division, Lawrence Berkeley National Laboratory, Berkeley, California 94720, USA*
[4]*Interdisciplinary Nanoscience Center (iNANO), Aarhus University, DK 8000 Aarhus C, Denmark*
[5]*Department of Materials Science and Engineering, University of California at Berkeley, California 94720, USA*

(Received 4 June 2012; accepted 14 December 2012; published online 11 January 2013)

The electronic structure of Cu_2O and CuO thin films grown on Cu(110) was characterized by X-ray photoelectron spectroscopy (XPS) and X-ray absorption spectroscopy (XAS). The various oxidation states, Cu^0, Cu^+, and Cu^{2+}, were unambiguously identified and characterized from their XPS and XAS spectra. We show that a clean and stoichiometric surface of CuO requires special environmental conditions to prevent loss of oxygen and contamination by background water. First-principles density functional theory XAS simulations of the oxygen K edge provide understanding of the core to valence transitions in Cu^+ and Cu^{2+}. A novel method to reference x-ray absorption energies based on the energies of isolated atoms is presented. © *2013 American Institute of Physics*. [http://dx.doi.org/10.1063/1.4773583]

I. INTRODUCTION

Copper and its oxides are widely studied because of their importance in many applications. These include catalytic processes such as methanol synthesis,[1,2] methanol steam reforming,[3,4] and NO_x reduction.[5] Copper oxides are promising photocatalysts for water splitting to produce H_2 under visible light irradiation.[6,7] They are also used as electrode materials in solar cells and lithium ion batteries.[8–10] Recently, several groups have studied low dimensional Cu oxide materials for applications as gas sensors.[11,12] Finally, copper oxide is an ideal model system to study strongly correlated electron phenomena in cuprate high-temperature superconductors.[13] To understand and improve these properties it is crucial to precisely determine the electronic structure of Cu in its various oxide forms, a task that is particularly important with regard to the oxide surface, where structure and composition play a crucial role in determining its properties.

X-ray photoelectron spectroscopy (XPS) and X-ray absorption spectroscopy (XAS) are powerful techniques to investigate the electronic structures of materials. In general, the probing depth of XAS in the fluorescence yield mode is larger than XPS due to the shorter mean free path of electrons compared with x-rays, which means XAS provides more bulk information. XAS can be made surface sensitive by operating in the electron yield mode where secondary electrons produced from the core-hole de-excitation are measured.[14] In the total yield mode (TEY) electrons of all energies are collected, whereas in partial yield mode (PEY) electrons in certain energy range are collected. There have been numerous X-ray spectroscopic studies of Cu in Cu_2O (cuprous) and in CuO (cupric) forms over the past decades.[15–38] However, due to instrumental limitations, it is difficult to combine XPS and XAS to characterize one sample under exactly the same conditions. As a result, for many XAS measurements the surface cleanliness is poorly known, while reported XPS peak positions in the literature vary also substantially,[21] which makes identification of the chemical state difficult. Another controversial issue in the O1s XPS spectra of oxide surfaces is the presence of additional features at the high binding energy side of the main peak, which are tentatively attributed to the formation of hydroxide or chemisorbed oxygen.[16,21]

From the theory and simulation perspective, CuO presents a challenge for standard density functional theory (DFT) due to its open-shell $3d^9$ electronic configuration, in contrast to the (nominally) closed-shell $3d^{10}$ Cu_2O. While both materials are semiconducting with band gaps of 1.3–1.7 eV[39,40] and 2.1 eV,[21] respectively, standard local and semi-local approximations to DFT underestimate the band gap of Cu_2O and render CuO a metal. Self-interaction corrected DFT studies have succeeded in opening a band gap

[a)]Current address: Dalian Institute of Chemical Physics, Chinese Academy of Sciences, 457 Zhongshan Road, Dalian 116023, China.
[b)]Current address: Canadian Light Source Inc., 44 Innovation Boulevard, Saskatoon, SK Canada, S7N 2V3.
[c)]Current address: Research Institute of Theoretical and Applied Physical Chemistry (INIFTA), National University of la Plata, CONICET, 1900 La Plata, Argentina.
[d)]Current address: Department of Chemistry and Biochemistry, University of Delaware, Newark, Delaware 19716, USA.
[e)]E-mail: MBSalmeron@lbl.gov.

in CuO (1.43 eV[41] or 2.2 eV[42]), while DFT with Hubbard potential (DFT+U) leads to a 1.48 eV (U = 7.0 eV) band gap.[43] In this work, we adopt the self-consistent linear response approach to DFT+U[44,45] to derive the Hubbard on-site correlation strength, U, for CuO.

Beyond ground state electronic structure we also simulate the x-ray absorption spectra using a constrained-DFT approach,[46] which has proved successful in predicting the K-edge spectra of both isolated and condensed phase systems.[47,48] Accurately reproducing the relative energies of excitation of different condensed phases in an efficient manner is desirable for both interpretation and prediction of measurements on chemically heterogeneous or dynamical systems. Recently, we have developed a new atomic alignment scheme[49] suitable for pseudopotential DFT calculations under periodic boundary conditions, which we apply here to estimate the x-ray absorption onset energies of both CuO and Cu_2O.

In this paper, we report studies on Cu_2O and CuO films grown on Cu(110). We show that by combining XPS and XAS techniques, careful energy calibration, and state-of-the-art XAS calculations, the identity and electronic structures of bulk and surface of Cu_2O and CuO can be determined unambiguously.

II. EXPERIMENTAL DETAILS

The experiments were performed using the ambient pressure photoemission endstation at beamline 11.0.2 of the Advanced Light Source in Berkeley.[50–52] The system consists of an ultrahigh vacuum (UHV) preparation chamber connected to an ambient pressure analysis chamber, where a combination of electrostatic focusing and differential pumping makes possible to collect XPS and XAS (partial electron yield) signals *in situ* at pressures of up to several Torr.

The Cu(110) single crystal used in this work was cleaned by cycles of Ar^+ sputtering and annealing until a sharp 1×1 LEED pattern was obtained and no contamination was observed by XPS. A Cu_2O thin film was prepared by thermal reduction (550 K) of a sacrificial CuO film formed by heating at 475 K for 10 min under 10 Torr of O_2. A new CuO film was later formed by thermal oxidation of Cu(110) under 1 Torr O_2 at 700 K. It should be noted that in order to avoid the hydroxylation and reduction of CuO, the XPS and XAS measurements were made under 1 Torr O_2 at 700 K, while for Cu and CuO_2 the spectra were measured under UHV conditions.

The photon energies used for XPS measurements of the O 1s and Cu 2p core levels were 835 eV and 1235 eV, respectively, which makes the kinetic energy (300 eV) of the photoelectrons the same for both species, thus ensuring a similar probing depth. Energy calibration is crucial for XPS because the photon energy and work function of the analyzer are parameters that might change in different experiments and in different ambient conditions. To address these issues an inert gold foil was mounted in electrical contact with the Cu sample and used as Refs. 53 and 54 by assigning the value of 84.0 eV and 335.0 eV to the binding energies of its $4f_{7/2}$ and $4d_{5/2}$ core levels. In the experiments reported here, 4f and 4d spectra were measured at each experimental condition using the same gas pressure, sample temperature, and beamline set-up parameters. The overall energy resolution is ± 0.1 eV.

Unfortunately the Au foil cannot be used as calibration standard for XAS measurements as it lacks sharp core level absorption edges in the soft- x-ray region. For that reason we used literature values of the Cu L_3 edge energies of 933.7 eV, 933.7 eV, and 931.3 eV, for metallic Cu, Cu_2O, and CuO, respectively, and 532.5 eV and 530.1 eV for the oxygen K edge in Cu_2O and CuO, respectively.[22,23,25] The kinetic energies for PEY mode were 500 eV and 300 eV for Cu L_3 and O K edges, respectively, with a pass energy set at 100 eV.

III. COMPUTATIONAL DETAILS

A. Ground-state electronic structure

Cu_2O is simulated in the bulk crystalline (antifluorite) phase with a 4.27 Å lattice constant. CuO is simulated using the structure and antiferromagnetic ordering outlined in Ref. 42 with lattice constants a = 4.68 Å, b = 3.42 Å, c = 5.13 Å, $\alpha = 90^\circ$, $\beta = 99.54^\circ$, $\gamma = 90^\circ$. Ultrasoft pseudopotentials[55] were employed under periodic boundary conditions and a plane-wave basis set with a kinetic energy cutoff of 31 Ry (33 Ry) for Cu_2O (CuO). The Cu sublattice pseudopotential is based on a core electronic configuration of $1s^2 2s^2 2p^6 3s^2 3p^6$ while the O pseudopotential employed a $1s^2$ core configuration. We use the generalized-gradient approximation of Perdew, Burke, and Ernzerhof[56] to the exchange-correlation potential. We employ the self-consistent linear response DFT+U approach[44,45] in the case of CuO, which would be (erroneously) metallic without the addition of on-site correlation which favors integer occupancy of localized electronic states (with Cu 3*d*-character in this case). We determined a self-consistent U = 4.5 eV, with a magnetic moment of 0.80 μ_B, which is an overestimate with respect to the experimental estimate of 0.64 μ_B, and an underestimated band gap of 0.8 eV. Electronic structure calculations were performed using the Quantum-ESPRESSO package.[57]

Currently, Cu $L_{2,3}$ edge simulations are not considered with our current XCH-DFT approach. We foresee that 2p core-level excitations of this kind can be modeled from first principles by solving the Bethe-Salpeter equation for electron-hole excitations with explicit inclusion of multiplet effects (although they may be quite small for these oxides). This approach has only been applied to early transition metal L-edges thus far.[58,59]

B. X-ray absorption simulations

The X-ray absorption spectra were simulated at the oxygen K-edge for both Cu_2O and CuO using constrained DFT under the excited electron and core-hole (XCH) approximation.[46] Currently, Cu $L_{2,3}$ edge simulations are not possible with our current XCH-DFT approach, as it cannot simulate multi-configurational excited states necessary to model the transition metal $L_{2,3}$-edges. Such strongly correlated excited states can be modeled from first principles by solving the Bethe-Salpeter equation for electron-hole excitations with explicit inclusion of multiplet effects, although this has only been applied to early transition metal L-edges

thus far.[58,59] The XCH approach uses a supercell impurity model to simulate the lowest energy core-excited state, by considering one excited atom within the supercell, whose ground-state pseudopotential is replaced with a core-excited pseudopotential (derived from the constrained electronic configuration $1s^1 2s^2 2p^5$ in the case of the oxygen atom) and the excited electron is placed in the first available unoccupied state. The electronic structure is relaxed under these constraints to model the final state and the resulting self-consistent-field used to derive the entire spectrum of higher excited states non-self-consistently. Transition matrix elements are calculated within the projector-augmented wave approximation[60] and the Fermi's Golden Rule expression for the X-ray absorption cross-section is accumulated. Efficient numerical convergence of the XAS is achieved with respect to Brillouin zone sampling using a generalized implementation[61] of the Shirley k-space interpolation scheme,[62] which was extended to include both electron spin and on-site Hubbard correlation, U. Lowest-energy core-excited states were simulated using core-hole pseudopotentials within supercells of 162 (192) atoms for Cu_2O (CuO) and spectra were converged by integration over a $5 \times 5 \times 5$ k-point grid.

C. Atomic alignment scheme

Accurate theoretical predictions of the x-ray absorption energies of materials are highly desirable, especially if we consider novel materials, or materials in novel environments (solvated, under bias, interfaced to another material, at high pressure, etc.) or potential impurities in a given sample. Each can present spectral features that have not yet been measured or interpreted. We recently derived a solution to this problem within the context of pseudopotential DFT calculations to compute accurate chemical shifts between various carbon-containing species solvated in water.[49] For clarity, we reintroduce this approach in the following paragraphs.

At present, DFT estimates of the absolute energies of x-ray core-level excitations are inaccurate and typically require *ad hoc* shifts to align with experiment. By choosing a reference system, greater accuracy can be achieved using relative energies, defined based on DFT total energy differences and associated cancelation of errors. In the past this approach has been employed to provide the relative spectral alignment for simulations of XAS from various molecular dynamics snapshots under constant volume and particle number.[46] In this context, even pseudopotential calculations could be used in the energy difference estimates, despite their lack of any absolute energy scale. However, if we wish to use pseudopotential calculations to provide accurate relative alignment between simulated spectra of completely different systems – gas vs. solid, or solid vs. solid as we have here – then we cannot rely on preserving either particle number or volume, and so, another scheme described next is required.

We define the relative first excitation energy of system (2) with respect to system (1), within our constrained-DFT approach, as

$$\Delta E = [E_{XCH}(2) - E_{GS}(2)] - [E_{XCH}(1) - E_{GS}(1)]. \quad (1)$$

This expression is valid within a pseudopotential context only if systems (1) and (2) share the same number of particles and system volume (under periodic boundary conditions). However, another set of energy differences, which are generally accurate (even with pseudopotentials) without such constraints, is atomization or formation energies. Let us consider the difference in atomization energy of the core-excited and ground states:

$$\begin{aligned}\Delta H_{XCH} - \Delta H_{GS} &= E_{XCH} - \left[\sum_{i\neq 0} \epsilon_{GS,i} + \epsilon_{XCH,0}\right] \\ &\quad - \left\{E_{GS} - \left[\sum_{i\neq 0} \epsilon_{GS,i} + \epsilon_{GS,0}\right]\right\} \\ &= [E_{XCH} - \epsilon_{XCH,0}] - [E_{GS} - \epsilon_{GS,0}],\end{aligned} \quad (2)$$

assuming that atom 0 is being core-excited, and atomic energies are indicated by $\epsilon_{GS,i}$, for atoms in their ground states, and $\epsilon_{XCH,i}$, for atoms in their core-excited states. One can unambiguously associate the core-excited state with only one atom from the original system, while the remaining ground state atoms drop out of the atomization energy difference. Notice that Eq. (2) also expresses a relative excitation energy between the total system and the isolated atom, as defined in Eq. (1). This energy difference is valid within the pseudopotential context as a difference in formation energies, even though it does not reflect a comparison between the excitation energies of systems with identical numbers and types of atoms. Therefore, having overcome this previous restriction, we can now reference the core-excitation energy of a given element in our chosen system to that of the isolated atomic element. If our atomic estimates are also performed under the same numerical constraints as the total system, viz. the same periodic boundary conditions, we also gain some cancelation of errors associated with our choice of numerical representation (number of plane waves or k-points, for example). In addition, by considering neutral excitations, we have relatively small finite-size errors associated with the spurious interaction between periodic images – at most, dipole-dipole interactions, which scale as the inverse of the supercell dimension to the third power. Note that it is this spurious interaction that limits our discussion in this work to reproducing the relative alignment of x-ray absorption spectra alone. On the contrary, the XPS final state is charged, and to compare systems with differing numbers of particles or supercell volumes, we would require corrections to our energy estimates to remove screened charge-charge interactions, which scale as the inverse of the supercell dimension. For isolated systems, where screening is absent at long-range, such corrections can be easily derived using the approach of Makov and Payne,[63] which has recently been demonstrated for a range of oxygen containing organic species.[64] We are currently working on addressing this issue for XPS chemical shift estimates beyond the gas phase, which must account for long-range screening contributions.

Finally, we choose an experiment on some system with a clearly defined spectral feature for a given element, and use the measured energy of that peak to align a constrained DFT estimate of the same core-excited system. For this work, we chose molecular gas phase O_2, which exhibits a strong π^* transition at 530.82 eV.[65] Our own simulation of the gas phase XAS of O_2 (not shown) agrees well with experiment and we determine a constant shift in energy to align the π^* peak after already shifting the O_2 spectrum with respect to our theoretically defined atomic O. This same constant is applied to both Cu_2O and CuO subsequent to their relative alignment to atomic O and the resulting aligned spectra are presented in Figure 2(a). Clearly, we achieve good agreement with the experimental spectra, which lacked an absolute energy reference but were aligned independently based on previous measurements.

IV. RESULTS AND DISCUSSION

A. X-ray photoelectron spectroscopy

Figure 1 shows the O 1s and Cu 2p core level XPS spectra of metallic Cu, Cu_2O, and CuO. The O 1s signal was absent in the metallic Cu spectrum indicating that, as expected, the surface is clean. The binding energy of O 1s is 530.3 eV for Cu_2O, and 529.4 eV for CuO. It is important to note that the CuO spectrum was acquired under 1 Torr O_2 at 700 K to maintain the stoichiometry of CuO as it tends to decompose in vacuum to Cu_2O at high temperature, while the high temperature is required to prevent species such as background H_2O from adsorbing onto the surface. The two peaks at around 538 eV are due to gas phase oxygen. A single O 1s XPS peak is observed for CuO, indicative of the cleanliness of the CuO surface. In previous studies a shoulder at about 1.8 eV higher binding energy from the main peak was attributed to hydroxyls produced by water adsorption.[16,21] The presence of O_2 gas makes the system closer to real working conditions as compared with high vacuum studies and is therefore of particular significance in studies of environment chemistry, photochemistry, and catalysis. We also noticed that when the sample was cooled to 375 K, a shoulder appeared around 531.0 eV, which coincides with the OH peak, as checked by dosing H_2O intentionally (data not shown). We did not observe a similar shoulder in the main peak for the O 1s spectra of Cu_2O after cooling, which indicates that the Cu_2O surface is more inert toward water than the CuO surface. A study of the different adsorption behavior of H_2O on CuO and Cu_2O surfaces will be reported separately.

In the Cu $2p_{3/2}$ core level XPS region we find the binding energies of Cu^0 and Cu^+ to be very similar, about 932.4 eV, while that of Cu^{2+} is 1.2 eV higher, at 933.6 eV. The full widths at half maximum of the Cu $2p_{3/2}$ spectra are also different for the three species: 2.8 eV for CuO, and 1.3 eV for both Cu and Cu_2O. Furthermore, for CuO a satellite feature is present at 942.0 eV that can be explained by the open $3d^9$ shell structure of Cu^{2+}. While it is more difficult to distinguish Cu^0 from Cu^+, analysis of the spectra in Fig. 1 reveals that Cu_2O (Cu^+) has small shake-up peaks at 946.0 eV and 938 eV. While the origin of the shake-up peaks is not yet understood it is clear that they are not present in metallic Cu. For all the three surfaces, the spin-orbit splitting separation between Cu $2p_{3/2}$ and $2p_{1/2}$ has the same value of 19.8 eV.

B. X-ray absorption spectroscopy

Figure 2 shows the O K-edge and the Cu $L_{2,3}$ XAS spectra normalized to the peak heights. The spectra are in good agreement with previous reports.[22,23,25,29] The oxygen XAS in CuO has a strong peak at 530.1 eV, which is attributed to transitions to conduction band states formed by hybridization of O 2p with Cu 3d electrons. The other features at higher energies involve hybridized O 2p orbitals with the Cu 4sp band. For Cu_2O, there is one prominent peak at 532.5 eV and minor features at higher energies.

Both CuO and Cu_2O have strong Cu L_3 absorption edges at 931.3 eV and 933.7 eV, respectively. Although it is interesting to correlate the absorption with core level binding energies, special care should be taken because of the uncertainty of the absolute values of the energies.[22,35] We notice that the incident X-ray photon energies are uncertain within

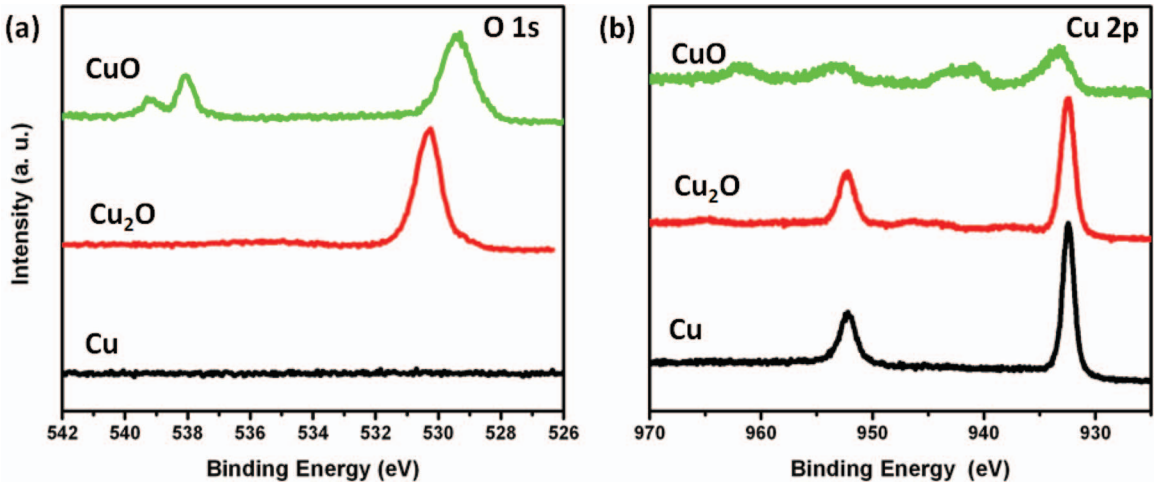

FIG. 1. (a) O 1s and (b) Cu 2p XPS spectra of Cu, Cu_2O, and CuO. To prevent loss of stoichiometry and water contamination, the CuO spectra were collected in the presence of 1 Torr O_2 at 700 K. For Cu and Cu_2O, the spectra were taken under UHV conditions.

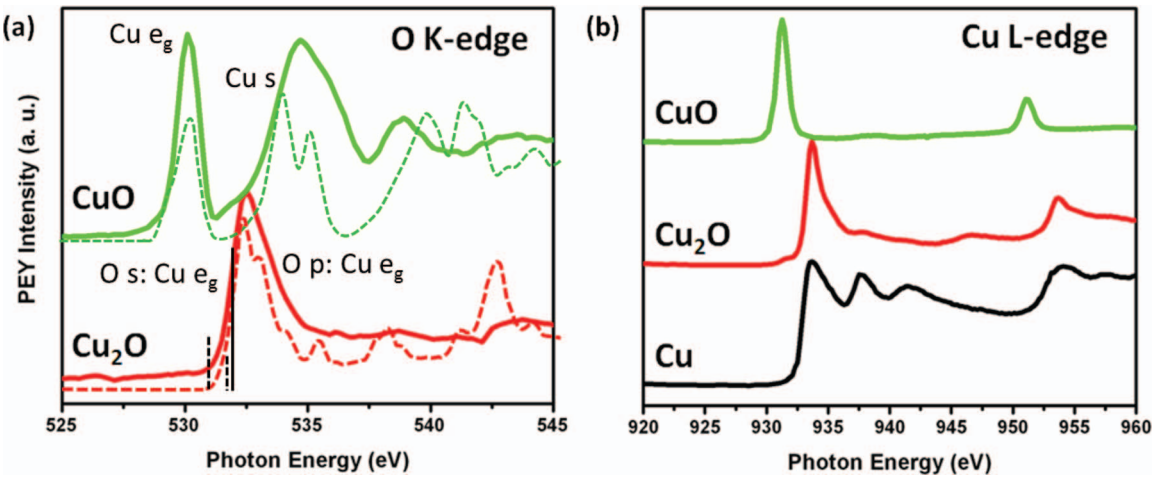

FIG. 2. (a) O K-edge and (b) Cu L-edge XAS spectra of Cu, Cu_2O, and CuO. Simulated O K-edge spectra obtained using the excited core hole DFT approximation are shown by dashed lines (see text for details), with the character of states contributing to each major peak indicated. Dark and bright excitons in Cu_2O are indicated by solid and dashed vertical lines, respectively.

$\pm$ 0.3 eV as a result of imprecise mechanical motion of the grating monochromator when changing photon energy, especially for measurements carried out at different beam times. However, the substantial shape differences between the XAS spectra of CuO and Cu_2O allow us to conclude that they can be unambiguously used as reliable fingerprints to identify oxide stoichiometry.

C. X-ray absorption simulations and interpretation

First-principles simulations of the x-ray absorption spectra of Cu_2O and CuO at the oxygen K-edge are reported as dashed lines in Figure 2(a). Spectral alignment is based on comparison of simulated XAS of an isolated O_2 molecule (not shown) with gas phase experimental data measured by Hitchcock and Mancini.[65] One can see immediately that excellent agreement with measurements is obtained. Upon resonant x-ray excitation, we find that the core-hole modified DOS shows an excitonic-like enhancement of features at the near-edge. Using a reduced spectral Gaussian convolution of 0.1 eV this produces sharp peaks at the oxygen K-edge for CuO, which could be of use in resonant inelastic scattering measurements to enhance the contribution to the x-ray emission. Analysis of the electronic component of the excitonic states shows that it involves coupling of O p-character to Cu e_g-character, at the bottom of the unoccupied Cu d_{x2-y2} band of the spin-minority channel. This is consistent with previous assignments.[23] The higher energy peak around 535 eV has been associated with Cu 4*s* character, however, integrated density of states shows that this peak also exhibits some Cu 3*d* character.

For Cu_2O, we find good agreement with the current and with previous measurements.[25] In that work, the projected density of states of Cu_2O was used to interpret spectral features, with assignments that agree with our own work. The asymmetry in the first peak was explained in Ref. 25 as resulting from core-hole attraction and approximated with an analytic final state rule. It is reproduced here with our XCH approach and at higher resolution we see an additional feature appear on the high-energy side of this peak, indicating some additional band structure beyond the conduction band minimum. This first peak results from hybridization between O 2*p* and Cu 3*d* (e_g) states.

Although states near the conduction band minimum have significant Cu d_{z2} or e_g character, the presence of O *s* character at the conduction band minimum of Cu_2O was already indicated in Fig. 2 of Ref. 25. At 530.9 and 531.6 eV in the simulated XAS we find two dark excitonic states, of O *s* character, lying 0.9 and 0.2 eV below the first, triply-degenerate bright transition (dashed and solid vertical lines in Fig. 2(a)), which may be detectable at elevated temperatures (to provide enough phonon coupling) or by X-ray Raman spectroscopy at large momentum transfer.

The calculated spectra show that the 2 eV oxygen chemical shift between Cu_2O and CuO is well reproduced using our isolated atomic reference scheme[49] as compared to the measured difference in absorption edges of 2.4 eV (Figure 2(a)). In addition, the absolute energy alignment (based on the O_2 molecule) is correct within 0.2 eV, indicating that our theoretical approach is both accurate and predictive.

V. CONCLUSIONS

The electronic structure of carefully prepared films of Cu_2O and CuO grown on Cu(110) surfaces has been investigated by XPS and XAS. *In situ* measurements in O_2 gas environments in the Torr pressure range and high temperature ensured that CuO was stoichiometric and close to thermodynamic equilibrium. By using the Au core level photoelectron energies as references to calibrate the energy scale, accurate binding energies of the elements present in the surfaces could be obtained for XPS. We have shown that the combination of XPS and XAS provides unambiguous identification of the various chemical species, while each technique alone would be less conclusive. Our results, together with the interpretation and energy alignment from density functional theory calculations using the XCH approach, provide the foundation for

further investigations of important copper oxide related applications and basic phenomena under different environmental and reaction conditions.

ACKNOWLEDGMENTS

This work was supported by the Director, Office of Science, Office of Basic Energy Sciences, Materials Sciences and Engineering Division, under the Department of Energy Contract No. DE-AC02-05CH11231. D.P. is funded by the Molecular Foundry. We also thank Dr. Jinghua Guo and Dr. Zhi Liu at the Advanced Light Source, for their helpful discussions.

[1]R. G. Herman, K. Klier, G. W. Simmons, B. P. Finn, J. B. Bulko, and T. P. Kobylinski, J. Catal. **56**, 407 (1979).
[2]J. C. Frost, Nature (London) **334**, 577 (1988).
[3]B. Lindström and L. J. Pettersson, Int. J. Hydrogen Energy **26**, 923 (2001).
[4]D. R. Palo, R. A. Dagle, and J. D. Holladay, Chem. Rev. **107**, 3992 (2007).
[5]G. Centi and S. Perathoner, Appl. Catal., A **132**, 179 (1995).
[6]M. Hara, T. Kondo, M. Komoda, S. Ikeda, K. Shinohara, A. Tanaka, J. N. Kondo, and K. Domen, Chem. Commun. **1998**, 357.
[7]P. E. de Jongh, D. V. Vanmaekelbergh, and J. K. Kelly, Chem. Commun. **1999**, 1069.
[8]B. P. Rai, Sol. Cells **25**, 265 (1988).
[9]C. M. McShane and K. S. Choi, J. Am. Chem. Soc. **131**, 2561 (2009).
[10]P. Poizot, S. Laruelle, S. Grugeon, L. Dupont, and J. M. Tarascon, Nature (London) **407**, 496 (2000).
[11]T. Ishihara, M. Higuchi, T. Takagi, M. Ito, H. Nishiguchi, and Y. Takita, J. Mater. Chem. **8**, 2037 (1998).
[12]J. Hu, D. D. Li, J. G. Lu, and R. Q. Wu, J. Phys. Chem. C **114**, 17120 (2010).
[13]J. M. Zuo, M. Kim, M. O'Keeffe, and J. C. Spence, Nature (London) **401**, 49 (1999).
[14]M. Abbate, J. B. Goedkoop, F. M. F. de Groot, M. Grioni, J. C. Fuggle, S. Hofmann, H. Petersen, and M. Sacchi, Surf. Interface Anal. **18**, 65 (1992).
[15]G. K. Wertheim and S. Hüfner, Phys. Rev. Lett. **28**, 1082 (1972).
[16]T. Robert, M. Bartel, and G. Offergeld, Surf. Sci. **33**, 123 (1972).
[17]G. Schön, Surf. Sci. **35**, 96 (1973).
[18]N. S. Mcintyre and M. G. Cook, Anal. Chem. **47**, 2208 (1975).
[19]M. R. Thuler, R. L. Benbow, and Z. Hurych, Z. Phys. Rev. B **26**, 669 (1982).
[20]S. L. Hulbert, B. A. Bunker, F. C. Brown, and P. Pianetta, Phys. Rev. B **30**, 2120 (1984).
[21]J. Ghijsen, L. H. Tjeng, J. van Elp, H. Eskes, J. Westerink, G. A. Sawatzky, and M. T. Czyzyk, Phys. Rev. B **38**, 11322 (1988).
[22]M. Grioni, J. B. Goedkoop, R. Schoorl, F. M. F. de Groot, J. C. Fuggle, F. Schäfers, E. E. Koch, G. Rossi, J. M. Esteva, and R. C. Karnatak, Phys. Rev. B **39**, 1541 (1989).
[23]F. M. F. de Groot, M. Grioni, J. C. Fuggle, J. Ghijsen, G. A. Sawatzky, and H. Petersen, Phys. Rev. B **40**, 5715 (1989).
[24]Z. X. Shen, R. S. List, D. S. Dessau, F. Parmigiani, A. J. Arko, R. Bartlett, B. O. Wells, I. Lindau, and W. E. Spicer, Phys. Rev. B **42**, 8081 (1990).
[25]M. Grioni, J. F. van Acker, M. T. Czyžyk, and J. C. Fuggle, Phys. Rev. B **45**, 3309 (1992).
[26]J. A. Rodriguez and J. Hrbek, J. Vac. Sci. Technol. A **12**, 2140 (1994).
[27]S. Poulston, P. M. Parlett, P. Stone, and M. Bowker, Surf. Interface Anal. **24**, 811 (1996).
[28]J. B. Reitz and I. Solomon, J. Am. Chem. Soc. **120**, 11467 (1998).
[29]M. Hävecker, A. Knop-Gericke, Th. Schedel-Niedrig, and R. Schlögl, Angew. Chem., Int. Ed. **37**, 1939 (1998).
[30]Th. Schedel-Niedrig, X. H. Bao, M. Muhler, and R. Schlögl, Ber. Bunsenges. Phys. Chem. **101**, 994 (1997).
[31]C. C. Chusuei, M. A. Brookshier, and D. W. Goodman, Langmuir **15**, 2806 (1999).
[32]A. B. Gurevich, B. E. Bent, A. V. Teplyakov, and J. G. Chen, Surf. Sci. **442**, L971 (1999).
[33]S. Y. Lee, N. Mettlach, N. Nguyen, Y. M. Sun, and J. M. White, Surf. Sci. **206**, 102 (2003).
[34]H. Bluhm, M. Hävecker, A. Knop-Gericke, E. Kleimenov, R. Schlögl, D. Teschner, V. I. Bukhtiyarov, D. F. Ogletree, and M. Salmeron, J. Phys. Chem. B **108**, 14340 (2004).
[35]J. P. Hu, D. J. Payne, E. G. Egdell, P. A. Glans, T. Learmonth, K. E. Smith, J. H. Guo, and N. M. Harrison, Phys. Rev. B **77**, 155115 (2008).
[36]X. Y. Deng, T. Herranz, C. Weis, H. Bluhm, and M. Salmeron, J. Phys. Chem. C **112**, 9668 (2008).
[37]S. L. Harmer, W. M. Skinner, A. N. Buckley, and L. J. Fan, Surf. Sci. **603**, 537 (2009).
[38]F. Yang, Y. M. Choi, P. Liu, J. Hrbek, and J. A. Rodriguez, J. Phys. Chem. C **114**, 17042 (2010).
[39]F. Mirabelli, G. B. Parravinci, and F. Salghetti-Driolli, Phys. Rev. B **52**, 1433 (1995).
[40]Y. S. Chaudhary, A. Agrawal, R. Shrivastav, V. R. Satsangi, and S. Dass, Int. J. Hydrogen Energy **29**, 131 (2004).
[41]A. Svane and O. Gunnarsson, Phys. Rev. Lett. **65**, 1148 (1990).
[42]A. Filippetti and V. Fiorentini, Phys. Rev. Lett. **95**, 086405 (2005).
[43]M. Nolan and S. D. Elliott, Phys. Chem. Chem. Phys. **8**, 5350 (2006).
[44]M. Cococcioni and S. de Gironcoli, Phys. Rev. B **71**, 035105 (2005).
[45]H. J. Kulik, M. Cococcioni, D. A. Scherlis, and N. Marzari, Phys. Rev. Lett. **97**, 103001 (2006).
[46]D. Prendergast and G. Galli, Phys. Rev. Lett. **96**, 215502 (2006).
[47]J. S. Uejio, C. P. Schwartz, R. J. Saykally, and D. Prendergast, Chem. Phys. Lett. **467**, 195 (2008).
[48]C. P. Schwartz, J. S. Uejio, A. M. Duffin, A. H. England, D. N. Kelly, D. Prendergast, and R. J. Saykally, Proc. Natl. Acad. Sci. U.S.A. **107**, 14008 (2010).
[49]A. H. England, A. M. Duffin, C. P. Schwartz, J. S. Uejio, D. Prendergast, R. J. Saykally, Chem. Phys. Lett. **514**, 187 (2011).
[50]M. Salmeron and R. Schlögl, Surf. Sci. Rep. **63**, 169 (2008).
[51]D. F. Ogletree, H. Bluhm, E. D. Hebenstreit, and M. Salmeron, Nucl. Instrum. Methods Phys. Res. **601**, 151 (2009).
[52]H. Bluhm, J. Electron Spectrosc. Relat. Phenom. **177**, 71 (2010).
[53]P. Jiang, S. Porsgaard, F. Borondics, M. Köber, A. Caballero, H. Bluhm, F. Besenbacher, and M. Salmeron, J. Am. Chem. Soc. **132**, 2858 (2010).
[54]S. Porsgaard, P. Jiang, F. Borondics, S. Wendt, H. Bluhm, F. Besenbacher, and M. Salmeron, Angew. Chem., Int. Ed. **50**, 2266 (2011).
[55]D. Vanderbilt, Phys. Rev. B **41**, 7892 (1990).
[56]J. P. Perdew, K. Burke, and M. Ernzerhof, Phys. Rev. Lett. **77**, 3865 (1996).
[57]P. Giannozzi *et al.*, J. Phys.: Condens. Matter **21**, 395502 (2009).
[58]E. L. Shirley, J. Electron Spectrosc. Relat. Phenom. **144-147**, 1187 (2005).
[59]R. Laskowski and P. Blaha, Phys. Rev. B **82**, 205104 (2010).
[60]M. Taillefumier, D. Cabaret, A.-M. Flank, and F. Mauri, Phys. Rev. B **66**, 195107 (2002).
[61]D. Prendergast and S. G. Louie, Phys. Rev. B **80**, 235126 (2009).
[62]E. L. Shirley, Phys. Rev. B **54**, 16464 (1996).
[63]G. Makov and M. C. Payne, Phys. Rev. B **51**, 4014 (1995).
[64]C. E. Patrick and F. Giustino, Phys. Rev. B **84**, 085330 (2011)
[65]A. P. Hitchcock and D. C. Mancini, J. Electron. Spectrosc. Relat. Phenom. **67**, 1 (1994).